Regeneration Rosetta: An interactive web application to explore regeneration-associated gene expression and chromatin accessibility

Andrea Rau[1,2], Sumona P. Dhara[3], Ava J. Udvadia[3], Paul L. Auer[2]

[1] GABI, INRA, AgroParisTech, Universite Paris-Saclay, 78350, Jouy-en-Josas, France
[2] Joseph J. Zilber School of Public Health, University of Wisconsin-Milwaukee, Milwaukee, WI 53201, USA
[3] Department of Biological Sciences, University of Wisconsin-Milwaukee, Milwaukee, WI 53201, USA

Abstract Time-course high-throughput assays of gene expression and enhancer usage in zebrafish provide a valuable characterization of the dynamic mechanisms governing gene regulatory programs during CNS axon regeneration. To facilitate the exploration and functional interpretation of a set of fully-processed data on regeneration-associated temporal transcription networks, we have created an interactive web application called *Regeneration Rosetta*. Using either built-in or user-provided lists of genes in one of dozens of supported organisms, our web application facilitates the (1) visualization of clustered temporal expression trends; (2) identification of proximal and distal regions of accessible chromatin to expedite downstream motif analysis; and (3) description of enriched functional gene ontology categories. By enabling a straightforward interrogation of these rich data without extensive bioinformatic expertise, *Regeneration Rosetta* is broadly useful for both a deep investigation of time-dependent regulation during regeneration in zebrafish and hypothesis generation in other organisms.

Keywords CNS axon regeneration; gene expression; chromatin accessibility; functional enrichment; zebrafish; R/Shiny

Introduction

Axon degeneration accompanying central nervous system (CNS) injury or disease leads to a permanent loss of function in human patients. This is largely due to an inability of mammals to reinitiate axon growth in adult CNS neurons (Crair and Mason 2016). In contrast to mammals, adult teleost fish can fully regenerate CNS axons that reinnervate appropriate targets, enabling functional recovery from CNS injury (Diekmann *et al.* 2015). Interestingly, fish and mammals

share common mechanisms for wiring the nervous system during development, and both are known to downregulate developmental growth and guidance signaling pathways during nervous system maturation (Skene 1989; Erskine and Herrera 2014). Thus, what appears to set fish apart is the ability to re-initiate a sustained program of axon growth in response to CNS injury.

Transcriptional changes have long been correlated with the intrinsic capacity for regenerative axon growth (Smith and Skene 1997; Moore and Goldberg 2011). In order to understand the precise mechanisms governing gene regulatory programs during CNS axon regeneration, Dhara et al. (2019) recently identified the dynamic changes in gene expression and enhancer usage in zebrafish over the full time-course of axon regeneration in CNS neurons that are capable of successful regeneration. Adult zebrafish were subjected to optic nerve crush injury, and regenerating retinas were dissected at various time-points post injury in order to identify the interactions among expressed genes, open chromatin, and transcription factor expression during CNS axon regeneration.

These data on regeneration-associated temporal transcription networks in zebrafish represent a rich source of information with wide potential use and insight for the broader regeneration community. To this end, we provide fully processed data from Dhara et al. (2019) in an interactive web application, *Regeneration Rosetta*, as a means to explore, visualize, and functionally interpret regeneration-associated gene expression and chromatin accessibility. Using either built-in lists of differentially expressed (DE) genes from Dhara et al. (2019) or user-provided gene lists in one of 69 supported organisms from Ensembl (Table 1), our web application facilitates (i) customized visualization of clustered temporal expression trends during optic nerve regeneration; (ii) identification of proximal and distal regions of open chromatin relative to the gene list to expedite downstream motif analysis via the MEME suite (Bailey *et al.* 2009); and (iii) gene ontology (GO) functional enrichment analysis. Similarly, using either built-in lists of differentially

accessible chromatin from Dhara et al. (2019) or user-provided genomic coordinates of accessible chromatin, the application identifies proximal and distal genes relative to their position and their corresponding enriched GO categories.

Species	Genome version	Species	Genome version
Danio rerio	GRCz10	*Meleagris gallopavo*	UMD2
Homo sapiens	GRCh38.p5	*Microcebus murinus*	micMur1
Mus musculus	GRCm38.p4	*Monodelphis domestica*	monDom5
Rattus norvegicus	Rnor_6.0	*Mustela putorius furo*	MusPutFur1.0
Ailuropoda melanoleuca	ailMel1	*Myotis lucifugus*	myoLuc2
Anas platyrhynchos	BGI_duck_1.0	*Nomascus leucogenys*	Nleu1.0
Anolis carolinensis	AnoCar2.0	*Ochotona princeps*	OchPri2.0
Astyanax mexicanus	AstMex102	*Oreochromis niloticus*	Oreni11.0
Bos taurus	UMD3.1	*Ornithorhynchus anatinus*	OANA5
Caenorhabditis elegans	WBcel235	*Oryctolagus cuniculus*	OryCun2.0
Callithrix jacchus	C_jacchus3.2.1	*Oryzias latipes*	HdrR
Canis familiaris	CanFam3.1	*Otolemur garnettii*	OtoGar3
Cavia porcellus	cavPor3	*Ovis aries*	Oar_v3.1
Chlorocebus sabaeus	ChlSab1.1	*Pan troglodytes*	CHIMP2.1.4
Choloepus hoffmanni	choHof1	*Papio anubis*	PapAnu2.0
Ciona intestinalis	KH	*Pelodiscus sinensis*	PelSin_1.0
Ciona savignyi	CSAV2.0	*Petromyzon marinus*	Pmarinus_7.0
Dasypus novemcinctus	Dasnov3.0	*Poecilia formosa*	PoeFor_5.1.2
Dipodomys ordii	dipOrd1	*Pongo abelii*	PPYG2
Drosophila melanogaster	BDGP6	*Procavia capensis*	proCap1
Echinops telfairi	TENREC	*Pteropus vampyrus*	pteVam1
Equus caballus	EquCab2	*Saccharomyces cerevisiae*	R64-1-1
Erinaceus europaeus	eriEur1		
Felis catus	Felis_catus_6.2	*Sarcophilus harrisii*	DEVIL7.0
Ficedula albicollis	FicAlb_1.4	*Sorex araneus*	sorAra1
Gadus morhua	gadMor1	*Sus scrofa*	Sscrofa10.2
Gallus gallus	Galgal4	*Taeniopygia guttata*	taeGut3.2.4
Gasterosteus aculeatus	BROADS1	*Takifugu rubripes*	FUGU4.0
Gorilla gorilla	gorGor3.1	*Tarsius syrichta*	tarSyr1
Ictidomys tridecemlineatus	spetri2	*Tetraodon nigroviridis*	TETRAODON8.0
Latimeria chalumnae	LatCha1	*Tupaia belangeri*	tupBel1
Lepisosteus oculatus	LepOcu1	*Tursiops truncatus*	turTru1
Loxodonta africana	loxAfr3	*Vicugna pacos*	vicPac1
Macaca mulatta	MMUL_1	*Xenopus tropicalis*	JGI4.2
Macropus eugenii	Meug_1.0	*Xiphophorus maculatus*	Xipmac4.4.2

Table 1. List of supported organisms and their associated genome version for user-provided gene set queries in the *Regeneration Rosetta* app.

The *Regeneration Rosetta* app represents a new paradigm to facilitate data sharing and re-use in the field of regeneration. This type of data sharing directly promotes the National Institutes of Health guidelines for ensuring rigor and reproducibility in pre-clinical research (https://www.nih.gov/research-training/rigor-reproducibility/principles-guidelines-reporting-

62 preclinical-researchas). As large-scale genomic data become more common, tools that allow
63 rapid querying and exploration of fully processed data (without the need for additional coding or
64 pre-processing steps) will be critical in accelerating advances in the regeneration field.

65 Materials and Methods

66 *Experimental design, data generation, and bioinformatic analyses*

67 Comprehensive experimental details may be found in Dhara et al. (2019). Briefly, whole retinas
68 were dissected from 7-9 month old adult zebrafish at 0, 2, 4, 7, or 12 days post injury (dpi),
69 following an optic nerve crush lesion (*n*=3 at each time point). For the RNA-seq data, we tested
70 differential expression with respect to the initial time point (0dpi), controlling the false discovery
71 rate at 5%. For the ATAC-seq data, sequences were aligned (Li and Durbin 2009) to the zebrafish
72 reference and open chromatin regions were called (Zhang *et al.* 2008). For each region with a p-
73 value < 10e-10, a 500bp "peaklet" was defined by anchoring on the mode of the peak signal
74 (Lawrence *et al.* 2013). Chromatin accessibility was quantified by counting the number of
75 overlapping reads for each retained peaklet, and differential accessibility was calculated with
76 respect to the initial time point (0dpi) (Love *et al.* 2014), controlling the false discovery rate at 5%.
77 Software versions and parameters are provided in Dhara et al. (2019). All genomic coordinates
78 and annotations are reported with respect to the GRCz10 Danio rerio genome assembly and
79 Ensembl 90 gene annotation for the zebrafish.

80 *Integration of RNA-seq and ATAC-seq data*

81

82 To link regions of accessible chromatin with gene expression, we calculated peaklet-to-gene
83 distance based on the coordinates of the peaklet mode and the gene's transcription start site
84 (TSS). A proximal peaklet was then defined as one that overlaps the TSS and/or is within ±1kb of
85 the TSS, while a distal peaklet was defined as one within ±100kb of the TSS but not proximal.

86 Users can optionally remove exonic peaklets from these lists, defined as those within 50bp of
87 exonic regions but not overlapping a TSS. To identify genes that are proximal or distal to a given
88 set of accessible chromatin (whether user-provided or through the built-in lists of differentially
89 accessible chromatin provided in the app), users may choose to include all genes or only a subset
90 of those identified to be DE at a particular time point.

91 For peaklets identified as proximal or distal to the query set of genes, a FASTA file of sequences
92 and BED file of genomic coordinates may be downloaded by the user for further analysis; in
93 addition, a CSV file providing the potentially many-to-many correspondences of proximal and
94 distal peaklets to genes may also be downloaded.

95 *Gene expression visualization and queries for alternative species*

96

97 Several built-in gene lists, based on the results described in Dhara et al. (2019), are directly
98 available within the *Regeneration Rosetta* app. These include the lists of DE genes (based on an
99 FDR adjusted p-value < 0.01) compared to 0dpi, as well as pre-identified clusters with expression
100 patterns roughly corresponding to established events in the regeneration process (down-
101 regulation during early-, mid-, or late-regeneration, growth toward the midline, midline crossing,
102 target selection, and brain innervation). Users may also employ the *Regeneration Rosetta* app to
103 explore gene sets for one of 68 species (Table 1) in addition to zebrafish by providing the relevant
104 Ensembl gene IDs (Durinck *et al.* 2009). These converted gene lists can be further narrowed to
105 include only those genes found to be DE post-injury.

106

107 For a given set of genes, expression heatmaps using log fold-changes, log transcripts per million
108 (TPM), or Z-scores of these measures are produced using *ComplexHeatmap* (Gu *et al.* 2016),
109 where transcript clusters are identified for a given number of clusters using the K-means
110 algorithm, and rows are ordered within each cluster according to hierarchical clustering (Euclidean

distance, complete linkage). Samples may also be hierarchically clustered. A high-resolution heatmap may be resized and downloaded by the user.

Functional enrichment analysis

The *Regeneration Rosetta* performs on-the-fly functional enrichment analyses of GO terms for Biological Processes (BP), Cellular Components (CC), and Molecular Function (MF) for a given gene set using *topGO* (`weight01` algorithm, Fisher test statistic, and gene universe defined as the set of expressed transcripts from Dhara et al. (2019). P-values are not adjusted for multiple correction, and only GO terms with raw p-values < 0.05 are reported; tables of enriched GO terms are displayed in an HTML table in the app and may be optionally downloaded as a CSV file, Excel spreadsheet, or PDF file. We remark that a list of enriched GO terms must be interpreted with respect to the context of the user-provided gene list. Most users of the *Regeneration Rosetta* would typically make use of lists of regeneration-related genes from one of the supported organisms to understand their behavior in the gene expression and chromatin accessibility data of Dhara et al. (2019); however, if provided with genes unrelated to regeneration, the app will typically return lists of enriched GO terms also unrelated to regeneration. We note that a variety of other ontology databases and enrichment methods exist in the literature, and the interested user could easily export a gene list obtained from the app to other tools, if desired.

Technical details of the Regeneration Rosetta

The *Regeneration Rosetta* interactive web app was built in R using the *Shiny* and *flexdashboard* packages. In addition to the other software packages already cited above, it makes use of the *data.table* and *RSQLite* R packages for fast data manipulation, *DT* for rendering HTML tables using JavaScript, *readxl* for parsing data from Excel spreadsheets, *dplyr* for data manipulation, and *tokenizers* to convert user-provided gene IDs into tokens. The *Regeneration Rosetta* R/Shiny

136 app is available at http://ls-shiny-prod.uwm.edu/rosetta/. A FAQ page is available directly on the
137 app website. Source code for the *Regeneration Rosetta* is available from GitHub:
138 https://github.com/andreamrau/rosetta. The processed data used within the app are directly
139 located in https://github.com/andreamrau/rosetta/tree/master/data; scripts used to process the
140 raw data from Dhara et al. (2019) may be found at
141 https://github.com/andreamrau/OpticRegen_2019. Archived source code at the time of
142 publication can be found at https://doi.org/10.5281/zenodo.2658771. The *Regeneration Rosetta*
143 app was developed under a GPL-3 software license.

144

145 **Results**

146 ***Regeneration Rosetta yields insight into cholesterol and lipid biosynthesis regulation***
147 ***during regeneration***

148 Cholesterol biosynthesis pathways were found to be enriched during regeneration in Dhara et al.
149 (2019) and have been previously shown to be important in axon regeneration in mouse (Wang *et*
150 *al.* 2018). To more deeply investigate their behavior during optic nerve regeneration in zebrafish
151 and demonstrate some of the capabilities of the *Regeneration Rosetta*, we input a list of 125
152 genes with cholesterol-related GO terms obtained from the Mouse Genome Informatics (MGI)
153 database (Smith *et al.* 2018) (Table S1), corresponding to 232 expressed zebrafish transcripts,
154 into the *Regeneration Rosetta* app (Fig. 1).

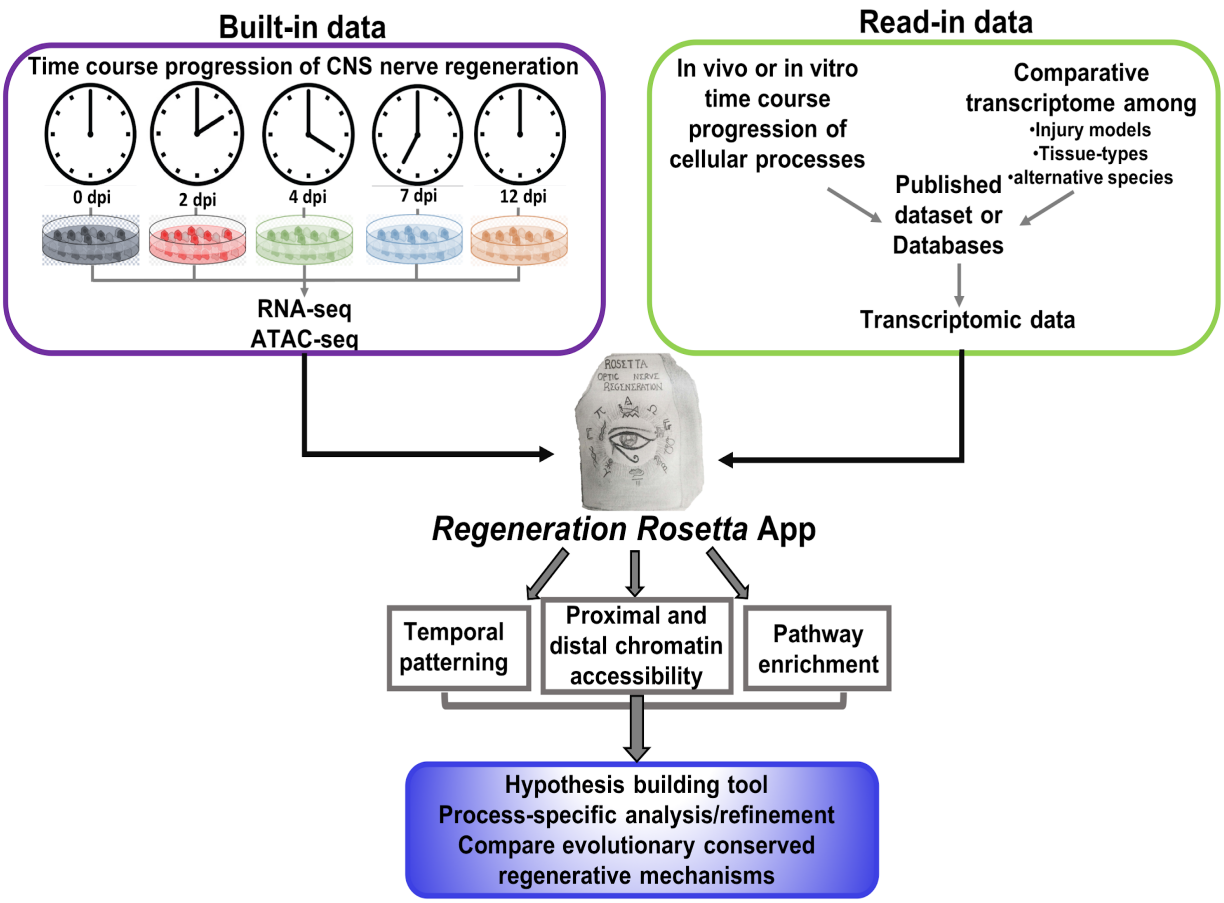

Figure 1: Workflow of *Regeneration Rosetta* app. Workflow for investigating temporal patterning of regeneration-associated genes classified within specific biological processes and/or comparative evolutionary analysis of the conserved mechanism among regenerative species, using the *Regeneration Rosetta* app.

Of these 232 transcripts, 62 were differentially expressed (DE) in Dhara et al. (2019); focusing on this subset of transcripts, the *Regeneration Rosetta* produces a clustered heatmap of expression Z-scores across distinct stages of optic nerve regeneration (Table S2; Figure 2A). Using on the associated GO terms from MGI, we found that the twenty transcripts with peak expression early in regeneration during the phase of growth towards the midline (2-4 dpi) were predominantly enriched in cholesterol metabolic genes, while the majority of those peaking during the midline crossing and target selection phases (4-7 dpi) were enriched in cholesterol biosynthetic pathways

168 (Figure 2B). Interestingly, transcripts differentially down-regulated during regeneration were
169 enriched in negative regulation of cholesterol biosynthetic processes.

170 Among the cholesterol biosynthetic genes, we observed upregulation during mid-regeneration (4-
171 7 dpi) of SREBF2, a known cholesterol master-regulatory transcription factor (Madison 2016;
172 Smith *et al.* 2018). After downloading the FASTA files of the sequences for peaklets proximal and
173 distal to the 62 DE cholesterol metabolic genes from the *Regeneration Rosetta*, AME motif
174 analysis (McLeay and Bailey 2010) revealed that mostly proximal open chromatin were enriched
175 in the SREBF2 motif resulting in 23% sequence enrichment. We found a number of genes with
176 temporal expression profiles similar to SREBF2 that are proximal to these accessible binding
177 sites, including *dhcr24*, *hmgcs1*, *hsd17b7*, *insig1*, *sqlea*, and *idi1* (Figure 2A). Interestingly, the
178 proximal and distal peaks of *srebf1*, which exhibited peak expression during brain reinnervation
179 (7-12 dpi), were also enriched for SREBF2 motifs; SREBF1 is a transcription factor related to
180 SREBF2 that is known to regulate genes involved in fatty acid synthesis and lipid homeostasis
181 (Ferré and Foufelle 2007; McLeay and Bailey 2010; Ye and DeBose-Boyd 2011), both of which
182 have been shown to be important for axon growth and myelination during neurogenesis (Salles
183 *et al.* 2003; Dietschy and Turley 2004; Ferré and Foufelle 2007). This suggests that SREBF2
184 could potentially regulate the transcriptional activity of SREBF1, which, in turn, promotes the
185 expression of genes associated with later regenerative processes.

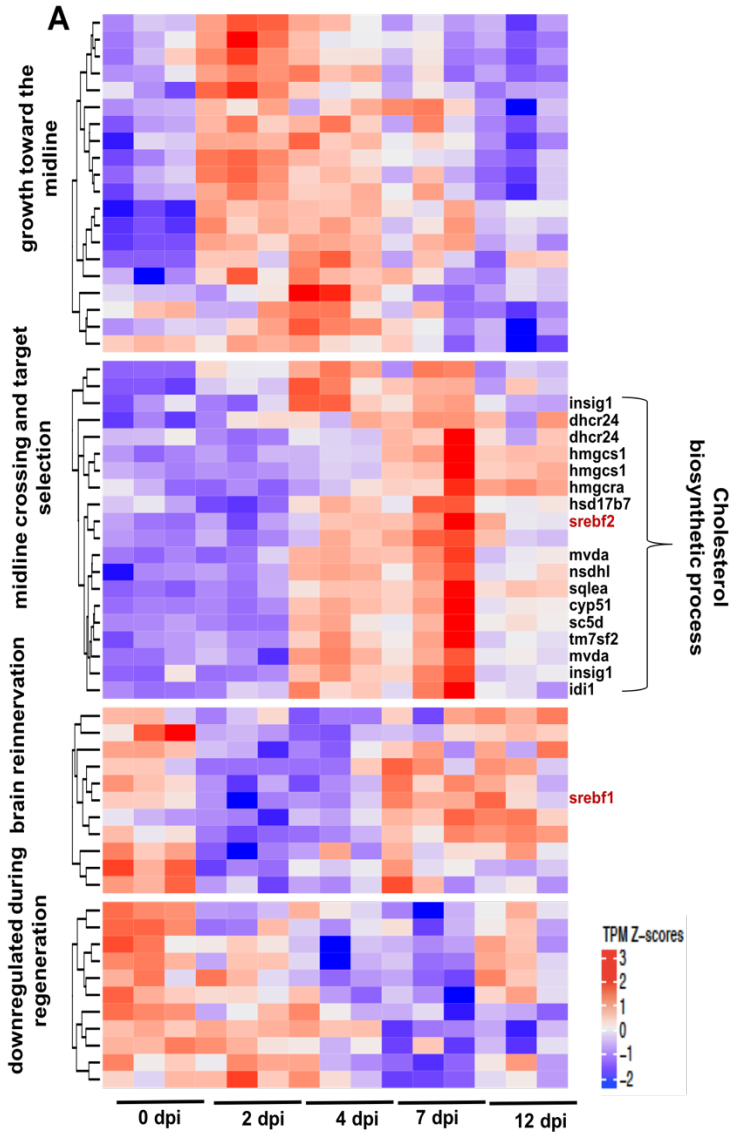
A
growth toward the midline
midline crossing and target selection
brain reinnervation
downregulated during regeneration
insig1
dhcr24
dhcr24
hmgcs1
hmgcs1
hmgcra
hsd17b7
srebf2
mvda
nsdhl
sqlea
cyp51
sc5d
tm7sf2
mvda
insig1
idi1
Cholesterol biosynthetic process
srebf1
TPM Z-scores
3
2
1
0
-1
-2
0 dpi
2 dpi
4 dpi
7 dpi
12 dpi

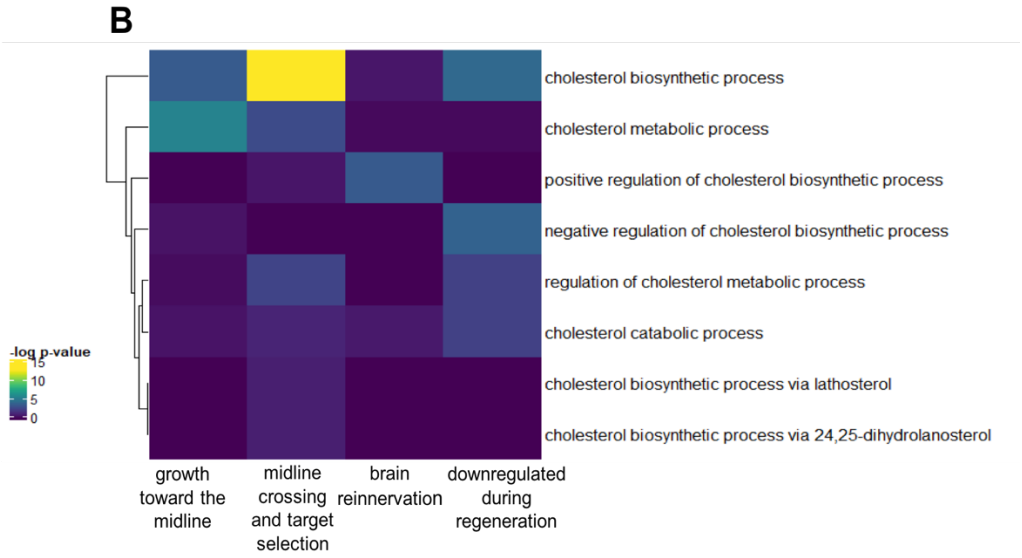
B
cholesterol biosynthetic process
cholesterol metabolic process
positive regulation of cholesterol biosynthetic process
negative regulation of cholesterol biosynthetic process
regulation of cholesterol metabolic process
cholesterol catabolic process
cholesterol biosynthetic process via lathosterol
cholesterol biosynthetic process via 24,25-dihydrolanosterol
-log p-value
15
10
5
0
growth toward the midline
midline crossing and target selection
brain reinnervation
downregulated during regeneration

186

187 **Figure 2: *Regeneration Rosetta* app identifies process-specific analysis after optic nerve injury**. (A)
188 Temporal transcript profiles of genes in the cholesterol metabolic pathway. Relative transcript counts from
189 retinas dissected 2-, 4-, 7- and 12-days post injury (dpi) were compared with those from uninjured animals
190 (0 dpi). Transcript expression is presented as TPM Z-scores; putative SREBF2 target genes are indicated
191 to the right of the heatmap (biosynthetic enzymes in black; transcription factors are in red). (B) Specific
192 enrichment of cholesterol metabolic and biosynthetic genes early in regeneration. Fisher's exact test of
193 over-representation was used to identify cholesterol-related GO-terms correlated with specific stages of
194 regeneration.

195 ***Regeneration Rosetta provides insight into evolutionary conserved regenerative***
196 ***mechanisms***

197 Nervous system function is dependent on the development of highly specific connections between
198 neurons and their direct targets. The molecular mechanisms regulating this network of
199 connections are highly conserved across evolution (Kaprielian *et al.* 2000; Jiang and Nardelli
200 2016). Unlike mammals, vertebrates such as fish and amphibians exhibit regenerative abilities of
201 complex tissues and structures. Therefore, comparing regenerative capabilities across species
202 will enable researchers to identify genes and transcriptional networks that are critical to the
203 regenerative program.

204 To facilitate a cross-species comparison, the *Regeneration Rosetta* app enables queries of
205 patterns of gene expression across injury models with different regenerative capacities. To
206 illustrate, we compared CNS regeneration in lamprey and zebrafish. Following (Kaprielian *et al.*
207 2000; Herman *et al.* 2018), we used the regenerating lamprey transcriptional profiles from cell
208 bodies located in the brain and spinal cord following spinal cord injury over a course of 12 weeks.
209 This study identified 3,664 and 3,998 differentially expressed regeneration-associated genes at
210 one or more post-injury time points in lamprey brain and spinal cord, respectively. After removing
211 duplicates, we filtered these lists to 2,325 (brain) and 2,519 (spinal cord) differentially expressed
212 genes. We looked for an overlap of genes that were differentially regulated after injury to the
213 zebrafish optic nerve and the lamprey brain and spinal cord. We found 3,712 transcripts
214 (corresponding to 2,150 genes) and 4,076 transcripts (corresponding to 2,404 genes) in the
215 zebrafish optic regeneration data corresponding to the lamprey brain and spinal cord,

216 respectively. After subsetting to those that were differential in the zebrafish (FDR <5%, Wald tests
217 vs 0dpi), we identified 734 (brain) and 846 (spinal cord) differentially expressed genes, 483 were
218 shared between the three data sets (Fig. 3). This suggests a considerable overlap between
219 responses to nerve injury in two different species and three different tissue types.

220 To identify the core transcription factors that could potentially regulate stage-specific
221 regeneration-associated gene transcription in both injury models, we cross referenced the
222 lamprey list of DE transcripts to a recently compiled list of human transcription factors (Lambert
223 *et al.* 2018). We identified 105 brain- and 131 spinal- transcription factor encoding genes that
224 were differentially expressed at one or more post-injury time points (Table S3 and S4). The
225 *Regeneration Rosetta* revealed 32 (brain) and 53 (spinal cord) DE transcription factor encoding
226 genes that were differential in the zebrafish optic nerve regeneration data after subjecting to FDR
227 5%, Wald tests vs 0dpi. Assessing the combined list of DE transcription factors, we found that 25
228 transcripts corresponding to 21 transcription factor encoding genes are shared among CNS
229 neuron responses to axonal injury in the lamprey spinal cord and brain, and zebrafish optic nerve
230 (Fig. 3). Thus, the *Regeneration Rosetta* highlights potential regulatory factors driving
231 regeneration-associated gene expression among regeneration capable organisms.

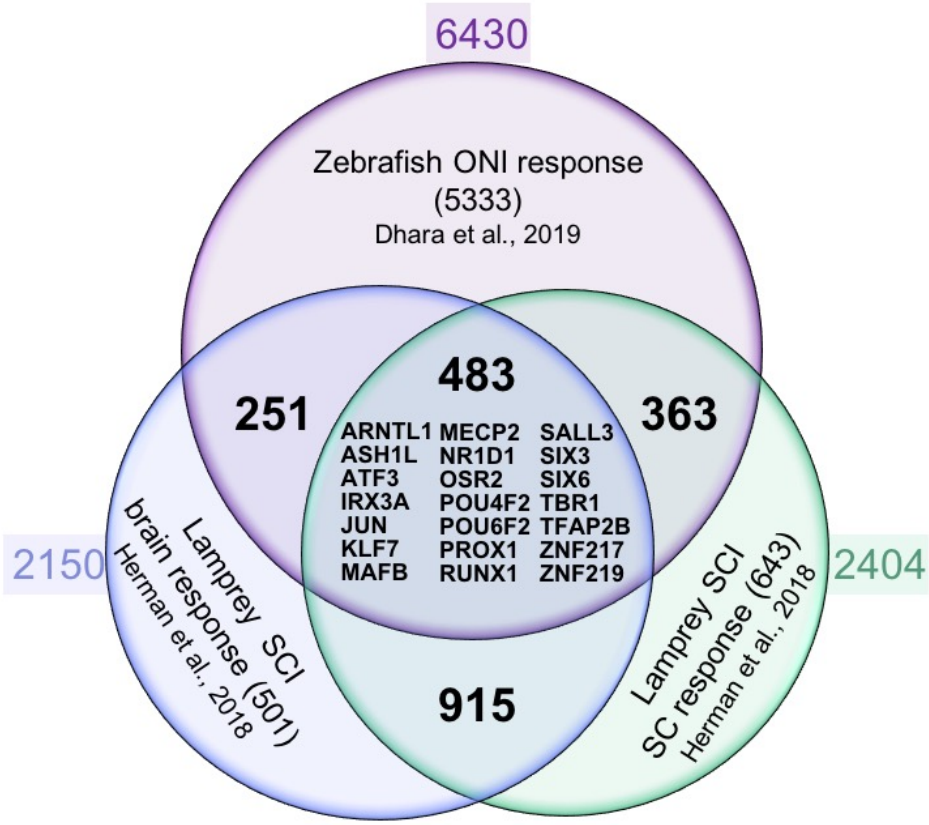

Figure 3. *Regeneration Rosetta* app identifies conserved core regulators of CNS axon regeneration. Venn diagram of axon growth-associated genes from regenerating CNS neurons after zebrafish optic nerve injury (ONI; retina response) and lamprey spinal cord injury (SCI; spinal cord (SC) and brain responses). Approximately 10-20% of regeneration-associated genes are shared between neurons regenerating axons in brain, spinal cord and optic nerve, including a core set of 21 regeneration-associated transcription factor encoding genes that are homologous to human genes (listed in the middle with HGNC gene symbol)

Discussion

The *Regeneration Rosetta* interactive web app represents a rich resource of fully processed, analyzed, and queryable data from a unique study of regeneration-associated gene expression and chromatin accessibility during optic nerve regeneration in Dhara et al. (2019). The app was a crucial component for generating and interpreting results in Dhara et al. (2019), as it facilitated a deep interrogation of the data that would have otherwise only been possible with extensive bioinformatic expertise. In addition, we have illustrated the broad utility of the *Regeneration Rosetta* app through examples focusing on time-dependent regulation during regeneration for

248 specific biological processes of interest and regenerative mechanisms that are evolutionarily
249 conserved across species and tissue types. All of the source code for running our analyses and
250 implementing the app is posted on GitHub; in this way researchers can modify the code for their
251 own applications or run a local version of the app if desired. As such, the *Regeneration Rosetta*
252 app (and its open-source code) provide a useful a framework for sharing results and data. The
253 *Regeneration Rosetta* app will be widely useful, both for further investigation and interpretation of
254 the data from Dhara et al. (2019) and for hypothesis generation in other organisms. Indeed, we
255 have provided example user-provided gene lists from a variety of published regeneration studies
256 into the app. The lists include regeneration-associated genes from 10 different cell/tissue types
257 from five different species. Our applications allows users to explore how the expression of these
258 genes may change over the course of optic nerve regeneration. We expect these use cases of
259 the app to inform the design of future functional studies that are crucial for translating basic
260 biological insights into new therapeutics for optic nerve injury.

261 **Acknowledgments**

262 We thank the UWM High Performance Computing (HPC) Service for computing resources used
263 in this work. We are grateful to Maria Replogle for comments on the manuscript. We wish to thank
264 the University of Wisconsin Biotechnology Center DNA Sequencing Facility, Madison for providing
265 RNA and ATAC sample sequencing facilities. We gratefully acknowledge support from the
266 Research Growth Initiative Grant -RGI (to P.L.A. and A.J.U.), University of Wisconsin-Milwaukee.
267 A.R. was supported by the AgreenSkills+ fellowship program, which received funding from the
268 EU's Seventh Framework Program under grant agreement number FP7-609398 (AgreenSkills+
269 contract). S.P.D. was supported by the Clifford Mortimer Distinguished Scholar Award, University
270 of Wisconsin-Milwaukee.

271

272 **Reference:**

273 Bailey, T. L., M. Boden, F. A. Buske, M. Frith, C. E. Grant *et al.*, 2009 MEME Suite: Tools for
274 motif discovery and searching. Nucleic Acids Res. 37: 202–208.

275 Bray, N. L., H. Pimentel, P. Melsted, and L. Pachter, 2016 Near-optimal probabilistic RNA-seq
276 quantification. Nat. Biotechnol. 34: 525–527.

277 Crair, M. C., and C. A. Mason, 2016 Reconnecting eye to brain. J. Neurosci. 36: 10707–10722.

278 Diekmann, H., P. Kalbhen, and D. Fischer, 2015 Characterization of optic nerve regeneration
279 using transgenic zebrafish. Front. Cell. Neurosci. 9: 1–11.

280 Dietschy, J. M., and S. D. Turley, 2004 Cholesterol metabolism in the central nervous system
281 during early development and in the mature animal. J. Lipid Res. 45: 1375–1397.

282 Dhara, S. P., Rau, A., Flister, M. J., Recka, N. M., Laiosa M. D., Auer, P.L., and Udvadia, A. J.
283 2019. Cellular reprogramming for successful CNS axon regeneration is driven by a
284 temporally changing cast of transcription factors. Scientific Reports *(in press)*

285 Durinck, S., Spellman, P. T., Birney, E. and Huber, W. 2009 Mapping identifiers for the
286 integration of genomic datasets with the R/Bioconductor package biomaRt. Nat. Protoc. 4,
287 1184–1191

288 Erskine, L. & Herrera, E., 2014 Connecting the retina to the brain. ASN Neuro 6 :
289 1759091414562107.

290 Ferré, P., and F. Foufelle, 2007 SREBP-1c transcription factor and lipid homeostasis: Clinical
291 perspective. Horm. Res. 68: 72–82.

292 Gu, Z., Eils, R. & Schlesner, M., 2016 Complex heatmaps reveal patterns and correlations in
293 multidimensional genomic data. Bioinformatics 32, 2847–2849

294 Herman, P. E., A. Papatheodorou, S. A. Bryant, C. K. M. Waterbury, J. R. Herdy *et al.*, 2018
295 Highly conserved molecular pathways, including Wnt signaling, promote functional
296 recovery from spinal cord injury in lampreys. Sci. Rep. 8: 1–15.

297 Jiang, X. & Nardelli, J., 2016 Cellular and molecular introduction to brain development.
298 Neurobiol. Dis. 92, 3–17.

299 Kaprielian, Z., R. Imondi, and E. Runko, 2000 Axon guidance at the midline of the developing
300 CNS. Anat. Rec. 261: 176–197.

301 Lambert, S. A., A. Jolma, L. F. Campitelli, P. K. Das, Y. Yin *et al.*, 2018 The Human
302 Transcription Factors. Cell 172: 650–665.

303 Lawrence, M., W. Huber, H. Pagès, P. Aboyoun, M. Carlson *et al.*, 2013 Software for
304 Computing and Annotating Genomic Ranges. PLoS Comput. Biol. 9: 1–10.

305 Li, H., and R. Durbin, 2009 Making the Leap: Maq to BWA. Mass Genomics 25: 1754–1760.

306 Love, M. I., W. Huber, and S. Anders, 2014 Moderated estimation of fold change and dispersion
307 for RNA-seq data with DESeq2. Genome Biol. 15: 1–21.

308 Madison, B. B., 2016 Srebp2: A master regulator of sterol and fatty acid synthesis1. J. Lipid
309 Res. 57: 333–335.

310 McLeay, R. C., and T. L. Bailey, 2010 Motif Enrichment Analysis: A unified framework and an
311 evaluation on ChIP data. BMC Bioinformatics 11:.

312 Moore, D. L., and J. L. Goldberg, 2011 Multiple transcription factor families regulate axon
313 growth and regeneration. Dev. Neurobiol. 71: 1186–1211.

314 Pimentel, H., N. L. Bray, S. Puente, P. Melsted, and L. Pachter, 2017 Differential analysis of

315 RNA-seq incorporating quantification uncertainty. Nat. Methods 14: 687–690.

316 Salles, J., F. Sargueil, A. Knoll-Gellida, L. A. Witters, C. Cassagne *et al.*, 2003 Acetyl-CoA
317 carboxylase and SREBP expression during peripheral nervous system myelination.
318 Biochim. Biophys. Acta - Mol. Cell Biol. Lipids 1631: 229–238.

319 Skene, J. H., 1989 Axonal growth-associated proteins. Annu. Rev. Neurosci. 12, 127–156.
320 doi: 10.1146/annurev.ne.12.030189.001015
321

322 Smith, C. L., J. A. Blake, J. A. Kadin, J. E. Richardson, and C. J. Bult, 2018 Mouse Genome
323 Database (MGD)-2018: Knowledgebase for the laboratory mouse. Nucleic Acids Res. 46:
324 D836–D842.

325 Smith, D. S., and J. H. Skene, 1997 A transcription-dependent switch controls competence of
326 adult neurons for distinct modes of axon growth. J. Neurosci. 17: 646–58.

327 Wang, Z., V. Mehra, M. T. Simpson, B. Maunze, A. Chakraborty *et al.*, 2018 KLF6 and STAT3
328 co-occupy regulatory DNA and functionally synergize to promote axon growth in CNS
329 neurons. Sci. Rep. 8: 1–16.

330 Ye, J., and R. A. DeBose-Boyd, 2011 Regulation of cholesterol and fatty acid synthesis. Cold
331 Spring Harb. Perspect. Biol. 3: 1–13.

332 Zhang, Y., T. Liu, C. A. Meyer, J. Eeckhoute, D. S. Johnson *et al.*, 2008 Model-based analysis
333 of ChIP-Seq (MACS). Genome Biol. 9:.

334